Received: Octber 30, 2016

INASS

International Journal of
Intelligent Engineering & Systems

http://www.inass.org/

Enhanced Isocentric Segmentor and Wavelet Rectangular Coder to Iris Segmentation and Recognition

Vanaja Roselin Emmanvelraj Chirchi[1*] **Laxman Madhavrao Waghmare[2]**

[1]*Jawaharlal Nehru Technological University, Kukatpally, Hyderabad, Telangana, India*
[2] *Shri Guru Gobind Singhji College of Engineering and Technology,Vishnupuri, Nanded, India*
*Corresponding author's Email: vanajaroselin1175@gmail.com

Abstract: In this paper, we propose a novel method for iris recognition system using enhanced isocentric segmentor (EISOS) and wavelet rectangular coder (WRC). At first, we locate the center of the eye within the area of the pupil on low resolution images using EISOS method. Once the iris region is successfully segmented, the next stage is to transform the iris region into the fixed dimensions. Then, we propose a novel feature vector generation method namely, wavelet rectangular coder (WRC). Finally, we recognize the iris image using fuzzy logic classifier to identify whether the iris image is present in the dataset or not. The iris recognition performance is measured using different dataset such as, CASIA, MMU and UBIRIS dataset. Experimental results indicate that the proposed method of EISOS+WRC based iris segmentation and recognition framework have outperformed by having better accuracy of 99.75% which is 94% and 93% for using existing approaches.

Keywords: Iris recognition; enhanced isocentric segmentor; wavelet rectangular coder; pupil; fuzzy logic classifier; iris segmentation.

1. Introduction

The expression "Biometrics" refers to a science concerning the statistical analysis of biological characteristics. Over the last decade, Biometric authentication has been obtaining wide attention with growing demands in automated personal identification. To recognize individuals is the plan of biometrics by means of physiological or behavioral characteristics such as fingerprints, face, iris, retina and palm prints. Iris recognition is one of the most hopeful approaches among many biometric techniques, due to its high dependability for personal identification [1]. In an iris recognition task, Iris segmentation is one of numerous major processing steps. To find out the valid region of the iris is the main objective of this iris segmentation step for recognition purposes [2]. Fundamentally this region is restricted by the pupil and sclera. In iris detection and recognition, feature extraction and selection are significant steps. An optimum feature set should have effectual and discriminating features, while mostly decrease the redundancy of features pace to evade "curse of dimensionality" problem [3]. Feature selection develops the precision of algorithms by decreasing the dimensionality and eliminating unrelated features. The main approach for iris recognition is to produce a feature vector which is related to individual iris images and to carry out iris matching based on some distance metrics. Diverse classification methods from statistical and machine learning area have been used for iris recognition. To identify the iris, many machine learning techniques have been used such as support vector machine (SVM), Haar wavelet transform, k-nearest neighbor (k-NN), daughman's algorithm, iris recognition by means of histogram analysis through LPQ and RI-LPQ method , Score Based Fusion Method [4], neural network [5], LBP and combined LBP classifier . The number of applications of organization and categorization, prediction, pattern recognition and control, neural networks model biological neural networks in the brain and have confirmed their competence.

Over the last few years, research in the area of iris recognition has been obtaining significant

attention and a number of methods and algorithms have been suggested. In 1987, Flom and Safir initially suggested the idea of automated iris recognition. Since then, several researchers have worked on iris representation and matching and have attained huge progress [6]. Boles and Boashash [7] worked out a zero-crossing representation of one-dimensional (1D) wavelet transform at different resolution levels of a concentric circle on an iris image to distinguish the consistency of the iris. Shufuxie et al. [8] made use of local Gabor XOR designs (LGXP) for recognition of face and iris modalities. Moreover, R. Valenti et al [9] planned to find the core of the eye inside the region of the pupil on low-determination images engaged from a web cam or a comparative gadget. Similarly, J. R. Sekar et al [10] have explained the Iris recognition based on the hybrid statistical and co-occurrence multi-resolution features. In the same way Radman et al [11] provided a rapid iris segmentation strategy. To control the access to limited places, Modern security sciences use these differences which are one of the basic problems in the security field. These conventional techniques can be forgotten, stolen, or cracked. For these weaknesses, the current science is concerned in automatic systems of recognition which are based on biometrics technology [12].

The main contributions of the paper are summarized as follows:

- **Segmentation:** To identify the pupil and iris region, we design a novel algorithm for segmentation namely, Enhanced Isocentric Segmentor (EISOS). In addition, EISOS gives an accurate eye center location in standard low resolution images with complete and fulfillment in segmentation structure.
- **Feature extraction:** To extract the suitable features for iris recognition system, we proposed a novel binary encoder scheme namely as, Wavelet Rectangular Coder (WRC). The binary encoder based on texture feature is suitable to do iris recognition; also, it can preserve the texture feature of the image by the neighborhood pixel replacement process for every block.

2. Proposed System for Iris Segmentation and Recognition

Biometric is a robotic technique, which is used for recognizing a person based on physiological or behavioral uniqueness. In this paper, we explain an iris based person authentication system using the combination of EISOS, WRC and fuzzy logic classifier. The flow diagram of proposed method is illustrated in figure 1. In this work, at first we segment the pupil and iris regions from the input image using the EISOS method. After the segmentation process, we extract the Iris code feature vector using WRC. Finally, the iris recognition is done through the fuzzy logic classifier.

2.1. Pupil and iris region Segmentation via EISOS method

The iris and pupil are very famous circular characteristics which are distinguished by an approximately stable intensity along the limbus (the junction between the sclera and the iris), and the iris and the pupil. In order to localize pupillary boundaries, the module of pupil segmentation is planned. A detailed description of the pupil segmentation procedures is explained below;

Stage 1: Image smoothing

Consider the gray scale eye image K_{gray}, which have some noises. To reduce the noise from the image, in our work, we utilize ***Gaussian*** smoothing methodology. Normally, smoothing is a process which is used to remove the noise present in the images. It is a 2-D convolution operator, which is used to 'blur' image and eliminate detail and noise from the input eye image K_{gray}. Moreover, which plays a significant function in edge detection in a human visual system, and amazingly valuable for edge and line detection.

Stage 2: Binary image generation

After image smoothing, the iris image is converted into a binary image which means, it converts an image of up to 256 gray levels to a black and white image. In binarization process, a threshold value is given to the input image and categorizes all pixels with values above this threshold as white, and all other pixels as black in image. Here, the binarization operation which is mentioned aims at identifying and isolating some regions of interest in the raw input image from its background. The threshold value used for generating the desirable binary image is automatically estimated in advance from the gray level histogram of the improved image.

$$B_{binary}(i,j)=\begin{cases} 0, & if\ K_{gray}(i,j)\le Threshold \\ 1, & Otherwise \end{cases} \quad (1)$$

Where, B_{binary} represents the obtained binary image and K_{gray} represents the input scale image.

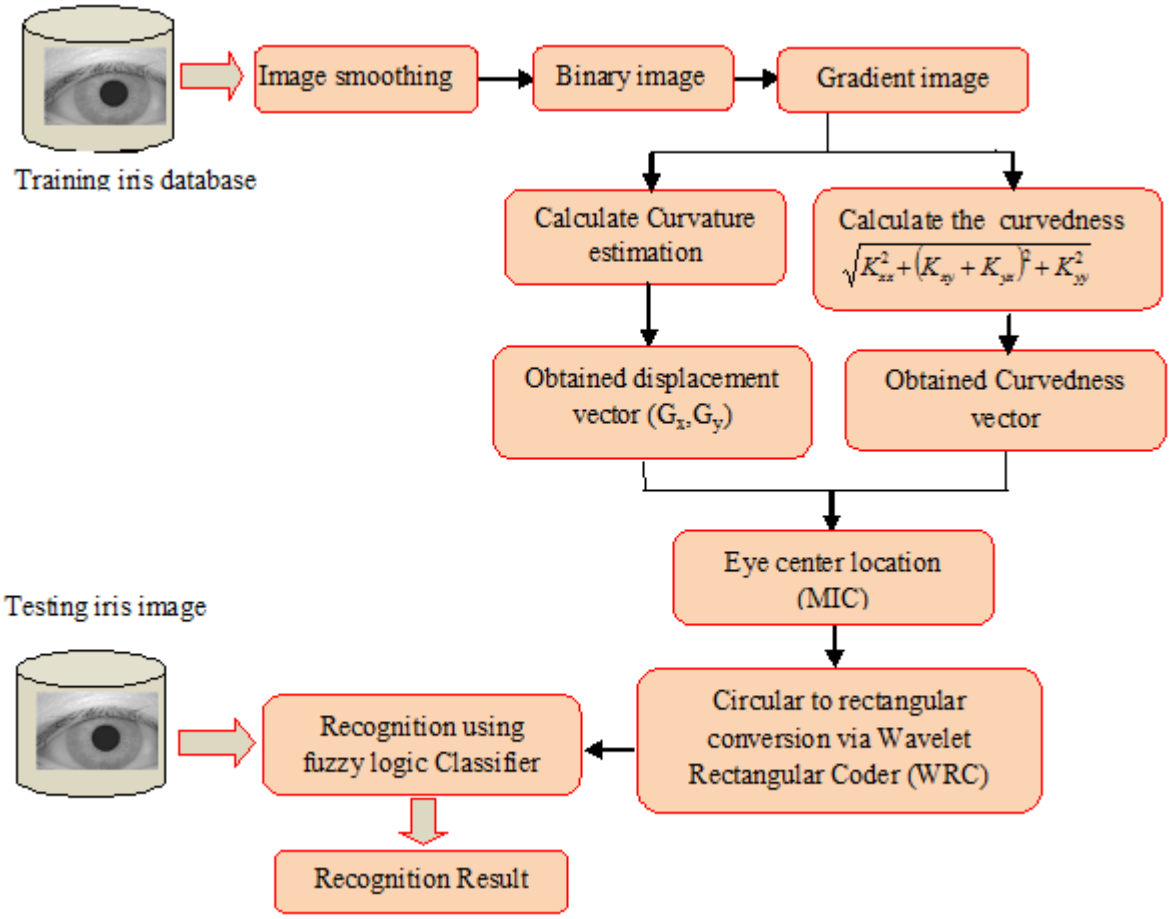

Figure.1 Overall diagram of Iris recognition

Stage 3: Isophotes curvature estimation

The aim of this section is to estimate the curvature of the image using isophotes curvature estimation method. The isophotes properties are mainly used for object detection and image segmentation. Mainly, the isophote curvature g is defined as the upright to the gradient and it is autonomous of the size of the gradient.

Consider the first and second derivatives in the x direction of an image K, which are indicated as, K_x and K_{xx} correspondingly. Here, the gradient vector of the first order derivatives explains the presence of an edge and also the second order derivative explains the gradient is maximal. To better illustrate the Isophotes framework, the notion of intrinsic geometry is introduced i.e., geometry with a locally defined coordinate system. The reference frame $\{a, b\}$ is also referred as the gauge coordinates. In a fixed coordinate system derivatives are worked out. The vector b is termed in the direction of the gradient and a is upright to b. Its frame vectors $\hat{a}$ and $\hat{b}$ are termed as:

$$\hat{b}=\frac{\{K_x, K_y\}}{\sqrt{|K_x^2+K_y^2|}} \qquad \hat{a}=\perp\hat{b} \tag{2}$$

Where, K_x and K_y are the first order derivatives of the luminance function $K(x,y)$ in x and y dimension, respectively. In this setting, a derivative in the b direction is the gradient itself, and the derivative in a direction (perpendicular to the gradient) is 0 (no intensity change along the Isophotes). In this coordinate system, the isophote is defined as $K(a,b(a))=constant$ and its curvature is defined as the change d^2b/da^2 of the tangent vector db/da. By implicit differentiation with respect to a of the Isophotes definition, we obtain:

$$\frac{db}{da}K_b+K_a=0\,; \qquad \frac{db}{da}=-\frac{K_a}{K_b} \tag{3}$$

$$\frac{db}{da}=-K_a K_b^{-1} \tag{4}$$

Since, $K_a=0$ from the gauge condition, then $(db/da)=0$. Therefore differentiating (3) once again respect to a, yields

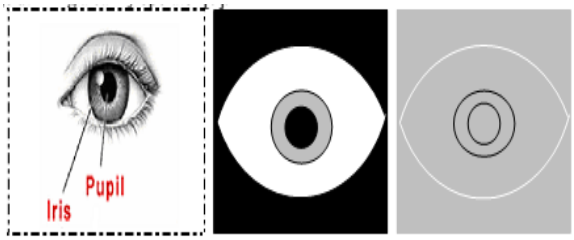

Figure.2 The original eye and notification of pupil and iris (a) and (b) isotopes curvature at the edges (c)

$$\frac{d^2b}{da^2} = -K_{aa}\,K_b^{-1} - K_b^{-1}\,K_{ab}\,\frac{db}{da} + K_a\,K_b^{-2}K_{ba} + K_a K_b^{-2}\,K_{bb}\cdot\frac{db}{da} = 0 \quad (5)$$

By considering the equation (3) we substitute the $g=K_{bb}$, $K_a=0$ and recall that $(db/da)=0$ the isophote curvature is obtained as

$$Isophote\ curvature\ g = -\frac{K_{aa}}{K_b} \quad (6)$$

Substituting equation (3) and (4) into (5) yield,

$$\frac{d^2b}{da^2} = -K_{aa}\,K_b^{-1} + K_b^{-1}\,K_{ab}\,K_a I_b^{-1} + K_a\,K_b^{-2}K_{ba} - K_a K_b^{-2}\,K_{bb}.K_a K_b^{-1} = 0 \quad (7)$$

$$= -K_{aa}K_b^{-1} + K_{ab}K_aK_b^{-2} + K_{ba}K_aK_b^{-2} - K_aK_{bb}K_b^{-3}K_a \quad (8)$$

$$= -\frac{K_{aa}K_b^2}{K_b^3} + 2K_{ab}K_aK_b^{-2} - \frac{K_a^2K_{bb}}{K_b^3} \quad (9)$$

The equation (8) in Cartesian coordinate it's given in equation (9).

$$g = -\frac{K_{aa}}{K_b} = -\frac{K_x^2\,K_{yy} - 2\,K_x K_{xy} K_y + K_x^2 K_{yy}}{\left(K_x^2 + K_y^2\right)^{3/2}} \quad (10)$$

where, $\{K_x,K_y\}$ and $\{K_{xx},K_{yy},K_{xy}\}$ are the first and second order derivatives of the luminance function $K(x,y)$ in the x and y dimensions respectively. From the equation (10), we obtain the isophotes curvature. To better representation of the eye image, a simplistic eye model is used, and is shown in figure 2 (a and b), the isophote curvature of the eye model is shown in figure 2(c). For presentation purposes, the indicated curvature fits in with the isophote under the edges found in the image utilizing a canny operator [9].

Stage 4: Center position estimation using displacement vector

After the isophote curvature estimation using above section stage 3, in this section, we calculate the center of the isophote. For every pixel, we are interested to retrieve the center of the circle which fits the local curvature of the isophote. We make out; the curvature is the reciprocal of the radius R; so equation (11) is turned around to attain the radius of this circle R.

$$R = \frac{1}{g} \quad (11)$$

The obtained radius magnitude is meaningless, if it is not compared with the orientation and direction. The orientation can be predictable from the gradient, but its direction will always point towards the highest change in the luminance as shown in figure 3 (a). However, the sign of the isophote curvature depends on the intensity of the outer side of the curve (for a brighter outer side the sign is positive). Accordingly, by multiplying the gradient with the contrary of the isophote curvature, the sign of the isophote curvature assists in disambiguating the direction to the center. As the unit gradient can be written as $\{K_x\,K_y\}/K_b$, we contain

$$\left(G_x, G_y\right) = \frac{\left(K_x, K_y\right)}{K_b}\left(-\frac{K_b}{K_{aa}}\right) = \frac{\{K_x,K_y\}}{K_{aa}} \quad (12)$$

$$= \frac{\{K_x,K_y\}\left(K_x^2 + K_y^2\right)}{K_y^2\,K_{xx} - 2\,K_x\,K_{xy}\,K_y + K_x^2\,K_{yy}} \quad (13)$$

Where, $\{G_x, G_y\}$ are the displacement vectors to the estimated position of the centers which can be mapped into an accumulator, hereinafter "center map". The set of vectors pointing to the estimated center is shown in figure 3(b). When compared to figure 3(a), it is possible to note that the vectors are now all correctly directed towards the center of the circular structures. Figure 3(c) represents the cumulative vote of the vectors for their center estimate (i.e. the accumulator).

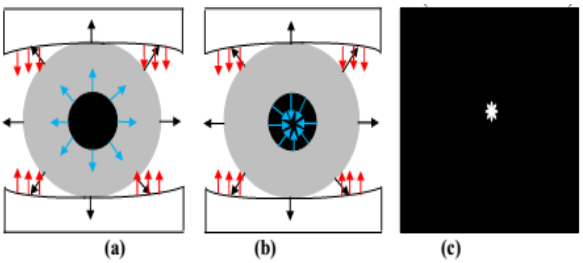

Figure.3 A detail showing the direction of the gradient underthe image's edges (a), the displacement vectors pointingto the isophote centers (b), and the centermap (c).

Stage 5: Center voting and eye center location

Reflect on the figure 3(a), we employ only three Isophotes; one explaining the pupil, another one explaining the iris and the final one explaining the boundary of the sclera. By convolving the eye model with Gaussian kernel, it can be examined that the number of isophotes increases around the edges as the steepness of the edge decreases, and that each of these new isophotes is same as the original isophotes, thus we employ to produce additional evidence to vote for right centerTo this conclusion, an image operator that points out how much a region diverges from flatness is required. This operator of the curvedness is defined in eq. (14) :

$$Curvedness = \sqrt{K_{xx}^2 + (K_{xy} + K_{yx})^2 + K_{yy}^2} \qquad (14)$$

The curvedness is regarded as a rotational invariant gradient operator, which calculates the degree of steepness of the gradient on the xy-axis and yx-axis and considering the sum of the pixel on x-y plane, this proposed equation(14) is acquiring all the pixel intensities of the iris so the feature pattern are clear for the further process . As a result, it gives up low response on flat surfaces and edges, while it yields high response around the edges. As isophotes are slices of the intensity landscape, there is a straight relation among the value of the curvedness and the density of isophotes. As a result, denser isophotes are possible to belong to the similar feature (i.e. edge) and hence locally agree on the similar center. By summing the votes, we attain high responses around the center of isocentric Isophotes patterns.

Table 1. The intermediate steps of the MIC determination

Steps	Image 1	Image 2
Input	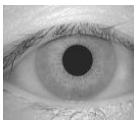	
Obtained center map	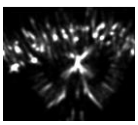	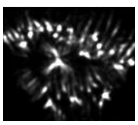
The edges that contributed to the vote of the MIC		
Segmented output		

The intermediate steps of the MIC determination are presented in table 1.

We name these high responses “isocenters”, or ICs. The maximum isocenter (MIC) in the center map will be employed as the most possible estimate for the sought after position of the center of the eye.

The MIC is calculated based upon the following condition

$$MIC = \begin{cases} C(i,j) & if\ G_x(i,j), G_y(i,j) > 0 \\ & and G_x(i,j), G_y(i,j) = T_l, \\ & T_l = L_B\ to\ U_B \\ 0 & otherwise \end{cases} \qquad (15)$$

Where, $G_x(i,j)$ is a Displacement vector at x direction and $G_y(i,j)$ is a Displacement vector at y direction

2.2 Circular to Rectangular Conversion via Wavelet Rectangular Coder (WRC)

Once pupil and iris regions are segmented using EISOS method, the feature extraction is performed using Wavelet Rectangular Coder (WRC) algorithm. At first, Daugman’s Rubber Sheet (DRS) Model is used to convert circular to rectangular conversion (CTRC) operation. After that, a rectangular iris image with the size of M×N is given to code generation process using WRC method. The detailed process of feature extraction scheme is presented below subsection:

- **Daugman’s Rubber Sheet Model**

Normalization process includes un-wrapping the iris and transforming it into its polar equivalent. It is performed utilizing Daugman’s Rubber sheet (DRS) model [14]. On polar axes, for each pixel in the iris, its equivalent position is found out. The process consists of two resolutions: (i) Radial resolution and (ii) Angular resolution. Utilizing the following equation, the iris region is transformed into a 2D array by making use of horizontal dimensions of angular resolution and vertical dimension of radial resolution.

$$I[x(r,\theta), y(r,\theta)] \rightarrow I(r,\theta) \qquad (16)$$

Where, $I(x,y)$ is the iris region, (x,y) and (r,θ) are the Cartesian and normalized polar coordinates respectively. The range of θ is $[0\ 2\pi]$ and r is $[0\ 1]$. $x(r,\theta)$ and $y(r,\theta)$ are described as linear combinations set of pupil boundary points. To perform the transformation, the formulas are given in the preceding equations

$$
\begin{aligned}
x(r,\theta) &= (1-r)x_p(\theta) + x_i(\theta), \\
y(r,\theta) &= (1-r)y_p(\theta) + y_i(\theta) \\
x_p(\theta) &= x_{p0}(\theta) + r_p Cos(\theta), \\
y_p(\theta) &= y_{p0}(\theta) + r_p Sin(\theta) \\
x_i(\theta) &= x_{i0}(\theta) + r_i Cos(\theta), \\
y_i(\theta) &= y_{i0}(\theta) + r_i Sin(\theta)
\end{aligned} \tag{17}
$$

Where, (x_p,y_p) and (x_i,y_i) are the coordinates on the pupil and iris boundaries along the θ direction.$(x_{p0},y_{po}),(x_{i0},y_{i0})$ are the coordinates of pupil and iris centers. This model gives a rectangular array with size of M×N image. Using this rectangular array, we are generating a binary code to form a feature set.

- **Wavelet Rectangular Coder (WRC)**

Once CTRC operation is done via DRS Model, the code generation process is performed using WRC algorithm. Here, the normalized rectangular block with fixed size of 256× 128 is given to the input of the WRC. After applying the WRC for each image, we obtain the feature vector size of 1×107. The step by step process of WRC algorithm is given below;

1) Let the original image (rectangular array) be denoted as $A(x,y)$, the LL band transformation image be denoted as $A_{LL}(x,y)$, the HL band transformation image be denoted as $A_{HL}(x,y)$, the LH band transformation image be denoted as $A_{LH}(x,y)$, and the HH band transformation image be denoted as $A_{HH}(x,y)$. The binary code of $A_{LL}(x,y)$ denoted as BC_{LL}, the binary code of $A_{HL}(x,y)$ is denoted as BC_{HL}, the binary code of $A_{LH}(x,y)$ is denoted as BC_{LH} and binary code of $A_{HH}(x,y)$ is denoted as BC_{HH}. The obtained single 8-bit binary code is denoted as B_S and the corresponding decimal value is denoted as D_B. The final output of the rectangular array image is represented as $A_{out}(x,y)$.
2) At first, the DWT is applied to the image $A(x,y)$, which will produce four sub- bands like LL, HL, LH, and HH. Subsequently, each sub bands are divided into set of blocks. Here, a set is represented as 3*3 blocks with center pixel X_c.
3) The main intention is to generate code from each 3*3 blocks to replace center pixel of the block, which will further replaced in image $A(x,y)$. To do this process, one condition is applied in each block X_c, based on its neighborhood to generate 8-bit binary code. The condition is given as follows:

$$
P_i = \begin{cases} 1 & for \;\; X_i > X_c \\ 0 & for \;\; otherwise \end{cases} \tag{18}
$$

Where,

P_i → i^{th} Pixel
X_c → Center block of the 3*3 block
X_i → i^{th} block

4) Based on the above condition, we generate the 8-bit binary code for each 3*3 blocks in every sub bands. Mathematically, the binary code generation can be represented as

$$
\begin{aligned}
BC_{LL} &\leftarrow [A_{LL}(x,y)]_{3\times3}, \\
BC_{HL} &\leftarrow [A_{HL}(x,y)]_{3\times3} \\
BC_{LH} &\leftarrow [A_{LH}(x,y)]_{3\times3}, \\
BC_{HH} &\leftarrow [A_{HH}(x,y)]_{3\times3}
\end{aligned}
$$

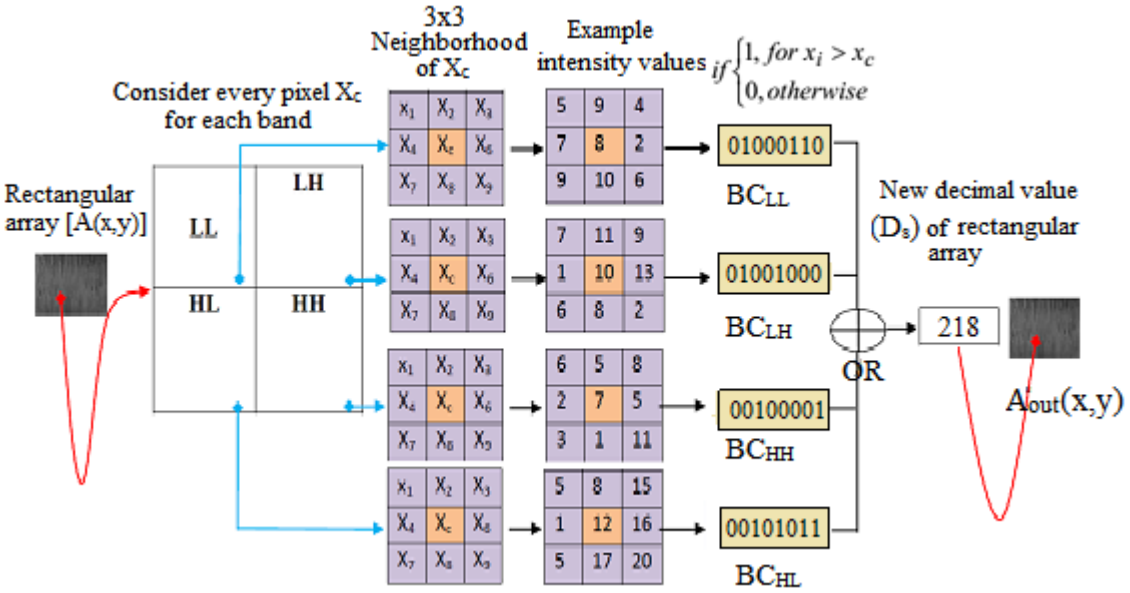

Figure.4 Process of the Wavelet Rectangular Coder

2.3 Iris Recognition using Fuzzy Logic Classifier

In this section, we have applied a fuzzy logic system using subtractive clustering for the recognition of two samples. To start the modeling process, an initial fuzzy model has to be derived. Fundamentally, fuzzy framework is characterized based on expert knowledge only. In a fuzzy classification system, an object can be classified by applying a set of fuzzy rules based on the linguistic values of its attributes. Here, genfis2 is utilized to initialize Fuzzy Interference System (FIS) training by applying the subtractive clustering [15] on the data. Using SUBCLUST function provided by MATLAB software to extract the set of rules that models the behavior of the data. To define the cluster centers, SUBCLUST function simply finds the optimal data point based on the density of the surrounding data points. In addition, this model is required to find the number of inputs, number of linguistic variables and hence the number of rules in the fuzzy model. The initial model is also required to select the input variables for the final model and also the model selection criteria. The system generates one output from N input. In this study, Gaussian membership function is used for the input data and triangular membership function is used for output data. In addition, the fuzzy rules are generated using subtractive clustering. Here, rule should have two different decisions like as YES and NO.

Recognition stage

The recognition of iris sample is carried out by using the fuzzy system designed in the previous sub-section. At first, the extracted features of test images T_S are given to the fuzzy logic system, in which the image features are converted into fuzzified value based on the fuzzy membership function. Then, the fuzzified input is matched with the fuzzy rules defined in the rule base. Here, the rule inference procedure is used to obtain the linguistic value then it is converted to the fuzzy score using the average weighted method. From the obtained fuzzy score, the decision is generated whether the test iris image belongs to the recognition or not.

3. Experimental Results

In this section, we discuss the result obtained from the proposed iris recognition system. For implementing the proposed approach, we have used MATLAB version 7.12. This proposed technique is done in windows machine having Intel Core i5 processor with speed 1.6 GHz and 4 GB RAM. In this experimental, we utilized the resized database images of size 128×128. For comparing the performance, we using three type of dataset such as CASIA, UBIRIS and MMU iris database

3.1 Evaluation Metrics

The evaluation of proposed iris recognition technique in bench mark database is carried out using the following metrics;

Accuracy: The Accuracy is the ratio of the total number of TP and TN to the total number of data.

$$Accuracy = \frac{TN + TP}{(TN + TP + FN + FP)}$$

where, FP represents the False positive, TP represents the True positive, TN represents the True negative and FN represents the False negative.

- **False Acceptance Rate (FAR):** FAR is the probability rate at which the numbers of iris images are erroneously received as Match.
- **False Rejection Rate (FRR):** FRR is the probability rate at which numbers of Iris images are erroneously received as “non-match”.

3.2 Dataset description

- **CASIA V1 dataset**

Chinese Academy of Sciences - Institute of Automation (CASIA) [5] is one of the database employed in the experimentation, eye image database encloses 756 grayscale eye images with 108 unique eyes or classes and 7 dissimilar images of each unique and the eye Size of each database iris image is 280x 320. As a result there is a total of 756 (108 x 7) images in the database. Since 2006, it has been liberated to more than 2,900 users from 70 countries or regions.

- **MMU dataset**

MMU1 iris database [4] contributes a total number of 450 iris images which were taken using LG IrisAccess®2200. On the other hand, MMU2 iris database consists of 995 iris images. The iris images are collected utilizing Panasonic BM-ET100US Authenticam and its operating period is even farther with a distance of 47-53 cm away from the user. These iris images are contributed by 100 volunteers with different age and nationality.

- **UBIRIS dataset**

Initially, under natural lighting and heterogeneous imaging conditions UBIRIS database [16] were incarcerated, which contains 10 photographs of each eye. The UBIRIS database has two separate versions such as ***UBIRIS.v1*** and ***UBIRIS.v2***. The ***UBIRIS.v1***

dataset contains 1 877 images gathered from 241 eyes during September 2004. The ***UBIRIS.v2*** dataset contains 11 000 images (and continuously growing) and more practical noise factors. Images were really incarcerated at-a-distance and on-the-move.

3.3 Experiment results on proposed approach

The performance of the proposed iris segmentation and recognition is analyzed with the help of FAR, FRR and accuracy, which are most significant performance parameters. In our experiment, we have taken 80% of dataset for training and remaining 20% for testing. The effectiveness of the proposed technique is demonstrated by performing a comparison between the matching result of the proposed method of EISOS+WRC and the conventional methods [17, 18, 19]. In this result part, we have the two phases such as segmentation phase and recognition phase.

- **Performance of Segmentation phase**

In segmentation phase, we use enhanced isocentric segmentor (EISOS) method, which is based on the curvature of the isophotes. In our work, we use two types of isophotes such as iris and pupil. The isophotes are cannot intersect each other and the images are fully described by its isophotes. Furthermore, the shape of the isophotes is independent to rotation and linear lighting changes [9].

Table 2. Visual representation of the segmentation phase

Input images	EISOS approach		Isocentric approach	
	The edges that contributed to the vote of the MIC	**Segmented Output**	**The edges that contributed to the vote of the MIC**	**Segmented Output**
				
				
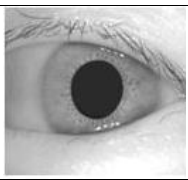		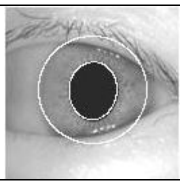	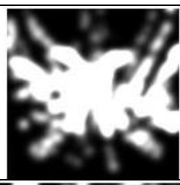	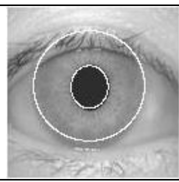
		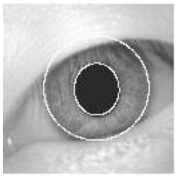	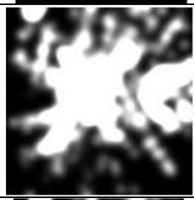	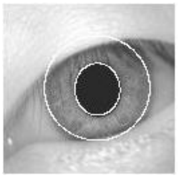
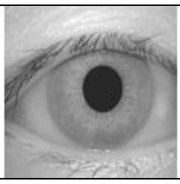	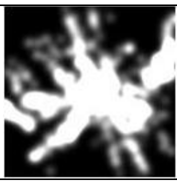	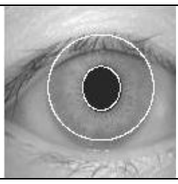	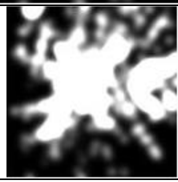	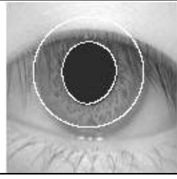

Table 3. Performance of segmentation phase using different database

Approaches	CASIA			MMU			UBIRIS		
	A	FRR	FAR	A	FRR	FAR	A	FRR	FAR
Isocentric approach [9]	80	7.3	0.44	79	7.5	0.48	78	7.7	0.46
EISOS-WRC (proposed)	87	0.07	0.36	86	0.09	0.41	85.5	0.08	0.43

Due to these properties, isophotes have been successfully used as features in object detection and image segmentation. The table 2 shows the visual representation of the segmentation phase and table 3 shows the Performance of segmentation phase using different database. When analyzing table 3, we obtain the accuracy of the proposed method is maximum for CASIA database, compared to MMU and UBIRIS database. Here, in our proposed approach achieve the overall segmentation accuracy of 87%; on other hand, the existing approach achieves only 80%. Moreover, from the table 6 we understand the error value of our approach is minimum compare to existing work [9].

- **Performance of Recognition phase**

The methods proposed by isocentric approach [9], PBIM based approach [17] SURF based approach [18] and Haar wavelet based approach [19] are the best known among existing schemes for iris recognition. Furthermore, they characterize local details of the iris based on phase, texture analysis, and local sharp variation representation. Therefore, we have chosen to compare the performance of our proposed algorithm against that of these. The isocentric approach [9] only works in segmentation phase; therefore we have not compared its performance because our method is proposed for a segmentation and recognition phase of operation. From the results shown in table 4, one can observe that [17] and our proposed one yield the best performances, followed by [18, 19]. This is because that these methods very well describe the texture features of the iris.

The below Table 4 shows the Performance analysis of Recognition phase based on the evaluation metrics such as FAR, FRR and accuracy. When analyzing table 7, we understand our proposed approach achieves the maximum accuracy of 99.75% but in [17, 18, 19] it achieves the accuracy value of 94%, 93% and 93.6 % respectively, for CASIA dataset.

Table 4. Performance of Recognition phase using different database

Approaches	CASIA			MMU			UBIRIS		
	A	FRR	FAR	A	FRR	FAR	A	FRR	FAR
PBIM approach [17]	94	0.06	0.04	93	0.06	0.04	92	0.06	0.05
SURF approach [18]	93	0.03	0.07	91	0.03	0.07	91	0.04	0.07
Haar wavelet based approach [19]	93	0.07	0.05	92	0.08	0.04	91	0.06	0.03
EISOS-WRC (proposed)	99	0.02	0	99	0	0.02	98	0.00	0.00

In [13], we obtain the accuracy of 94% by varying the parameters K_1/M_1 =0.4, 0.45, 0.5 and K_2/M_2 =0.2, 0.3. In [18] we obtain the accuracy of 93% on the CASIA database and [19] we obtain the accuracy of 93.6% for varying hamming distance. Also table 7, explains the FAR and FRR rate of three different dataset. Moreover, table 8 shows the performance of recognition phase based on feature extraction approach.

4. Conclusion

Iris segmentation is likely a standout amongst the most critical operations included in iris recognition. Exact iris segmentation is major for the precision and accuracy of the ensuing feature extraction and recognition. In this paper, we utilized EISOS approach based isophote properties for segmentation part to locate the center of the eye within the area of the pupil. A broad assessment of the proposed segmentation methodology was performed, testing it for accurate eye location in standard low determination images. The utilization of isophotes yields low computational cost and robustness to rotation and direct illumination changes. After that, we developed a new feature extraction algorithm called as WRC which is used to generate the unique features and reduce the partial occlusion present in the images. Finally, we adapted the iris recognition system based on the fuzzy logic classifier. Experimental results indicate that the proposed method of EISOS+WRC for iris segmentation and recognition framework have outperformed by having better accuracy of 99.75%. In future works, we will hybrid two or more classifiers for recognize to achieve better result. Also, the system should be tested on a larger

database to validate the robustness of the system.

References

[1] L. Ma, T. Tan, Y. Wang and D. Zhang, "Efficient Iris Recognition by Characterizing Key Local Variations", *Journal of IEEE Transaction Image Processing*, Vol. 13, No. 6, pp. 739-750, 2004.

[2] J. Daugman, "New methods in iris recognition", *Journal of IEEE Transactions on Systems*, Vol. 37, No. 4, pp. 1167-1175, 2007.

[3] A. Osareh and B. Shadgar, "A Computer Aided Diagnosis System for Breast Cancer", *International Journal of Computer Science*, Vol. 8, No. 2, pp. 233-235, 2011.

[4] Multimedia University, MMU iris image database, *http://pesona.mmu.edu.my/ccteo*.

[5] CASIA iris database, *http. // www.sinobiometrics.com/casiairis.htm*

[6] R. Wildes, J. Asmuth, G. Green, S. Hsu, R. Kolczynski, J. Matey and S. McBride, "A machine-vision system for iris recognition", *Journal of machine vision and applications*, Vol. 9, No. 1, pp. 1-8, 1996.

[7] W. Boles and B. Boashash, "A Human Identification Technique Using Images of the Iris and Wavelet Transform", *IEEE Transaction of Signal Processing*, Vol. 46, No. 4, pp. 1185-1188, 1998.

[8] S. Xie, S. Shan and X. C. J. Chen, "Fusing Local Patterns of Gabor Magnitude and Phase for Face Recognition", *IEEE Transactions on Image Processing*, Vol. 19, No. 5, pp. 1349-1362, 2010.

[9] R. Valenti and T. Gevers, "Accurate Eye Center Location through Invariant Isocentric Patterns", *Journal of IEEE transactions on pattern analysis*, Vol. 34, No. 9, pp. 1785-1798, 2012.

[10] J. R. Sekar, S. Arivazhagan, S. S. Priyadharshini and S. Shunmugapriya, "Iris recognition using combined statistical and co-occurrence multi-resolution features", *International Journal of Pattern Recognition*, Vol. 27, No. 1, 2013

[11] A. Radman, K. Jumari and N. Zainal, "Fast and reliable iris segmentation algorithm", *IET Image Processing*, Vol. 7, No. 1, pp. 42-49, 2013.

[12]B. Fang and Y. Y. Tang, "Elastic registration for retinal images based on reconstructed vascular trees", *IEEE Transaction on Biomedical Engineering*, Vol. 53, No. 6, pp. 1183-1187, 2006.

[13] J. Koenderink and A. J. van Doorn, "Surface shape and curvature scales", *Image and Vision Computing*, Vol. 10, No. 8, pp. 557-565, 1992.

[14] S. U. Maheswari, P. Anbalagan and T. Priya, "Efficient Iris Recognition through Improvement in Iris Segmentation Algorithm", *International Journal on Graphics, Vision and Image Processing*, Vol. 8, No. 2, pp. 29-35, 2008.

[15] S. Chiu, "Fuzzy model identification based on cluster estimation", *Journal of Intelligent & Fuzzy Systems*, Vol. 2, No. 3, pp. 267-278, 1994.

[16] UBIRIS iris image database, *http://iris.di.ubi.pt/*

[17] K. Miyazawa, K. Ito, T. Aoki, K. Kobayashi and H. Nakajima, "An Effective Approach for Iris Recognition Using Phase-Based Image Matching", *IEEE transactions on pattern analysis*, Vol. 30, No. 10, pp. 1741- 1756, 2008.

[18] H. Mehrotra, P. K. Sa and B. Majhi, "Fast segmentation and adaptive SURF descriptor for iris recognition", *Mathematical and Computer Modelling*, Vol. 58, No. 1, pp. 132-146, 2013.

[19] A. Panganiban, N. Linsangan and F. Caluyo, "Wavelet-based Feature Extraction Algorithm for an Iris Recognition System", *Journal of Information Processing Systems*, Vol. 7, No. 3, pp. 425-434, 2011.